

Horizontal movements in the eastern Barents Sea constrained by numerical models and plate reconstructions

Susanne J. H. Buiter and Trond H. Torsvik*

Centre for Geodynamics, Geological Survey of Norway, Leiv Eirikssons vei 39, 7491 Trondheim, Norway. E-mail: susanne.buiter@ngu.no

Accepted 2007 August 22. Received 2007 August 22; in original form 2007 April 13

SUMMARY

The eastern Barents Sea basins, west of Novaya Zemlya, were mildly inverted between Late Permian and Early Jurassic times, as indicated by mild folds in the basin sediments. Previous studies have suggested that the crustal part of Novaya Zemlya was thrust westward, but the magnitude of this compressive movement is not well known. Our aim is to provide an order-of-magnitude constraint on the amount of shortening associated with the displacement of Novaya Zemlya and inversion of the eastern Barents Sea basins by combining numerical models and plate reconstructions in an iterative process. We use a 2-D finite-element method to model inversion of a pre-defined basin. The total amount of shortening imposed on the models is first constrained by plate reconstructions for the Barents Sea region for the Late Palaeozoic to Early Mesozoic. We assume that the shortening is caused by westward movement of the Siberian plate, but the magnitude of this westward displacement in plate reconstructions is highly uncertain due to the allochthonous nature of the rocks of Novaya Zemlya and the scarcity of palaeomagnetic data in the region. Our models show that shortening localizes in the model basin and at Novaya Zemlya and that westward propagation of deformation is more efficient when the strength of the lower crust is reduced. Part of the movement of the Siberian plate could be accommodated by thrusts at Novaya Zemlya and perhaps in the domain of the Kara Sea at the western margin of the Siberian plate. By comparing the inversion obtained in the numerical models to the inferred inversion structures in the eastern Barents Sea basins we further constrain the amount of shortening that caused the inversion and therewith improve the plate reconstructions for the region. Our models indicate that the westward movement of Novaya Zemlya occurred in the Late Triassic–Early Jurassic (220–190 Ma) and was limited in magnitude to 100–200 km, which is considerably less than previous estimates (500–700 km).

Key words: Barents Sea, basin inversion, finite element model, Novaya Zemlya, plate reconstruction.

1 INTRODUCTION

Reconstructions of the position of tectonic plates through Earth's history help constrain the amount of convergence and divergence associated with plate margin processes and thus of contractional and extensional velocities. Such velocities can vary considerably from almost zero to high values as, for example, 14 cm yr⁻¹ for the Late Cretaceous Pacific–Eurasia convergence (Northrup *et al.* 1995) and 18–21 cm yr⁻¹ in the middle Miocene at the East Pacific Rise (Wilson 1996). The displacement magnitudes and velocities obtained from plate reconstructions can be used as a first order constraint on numerical models of plate margin behaviour. The velocity magnitudes are thereby also a control on viscous material strength

and can thus affect the style of deformation. However, plate reconstructions can in general not be used to constrain the amount of extension or shortening exactly. They are often based on palaeomagnetic data which have uncertainties caused by errors in the palaeomagnetic measurements, the distribution of measurement points and the fact that palaeomagnetic methods cannot be used to determine palaeolongitudes of continents or blocks. The uncertainty in continent positions generally increases backward in time and could be on the order of several hundreds of kilometres for the Mesozoic and Palaeozoic. The quantification of the displacements can, however, be improved through combination with other methods, as, for example, cross-section restoration or crustal thickness determination from seismic and seismological data. In this study, we combine plate reconstructions with numerical models. Our aim is to improve constraints on the amount of shortening associated with the inversion of the basins in the eastern Barents Sea, offshore of Novaya Zemlya (Fig. 1).

*Also at: PGP, University of Oslo, 0316 Oslo, Norway, and the School of Geosciences, University of Witwatersrand, WITS 2050, South Africa.

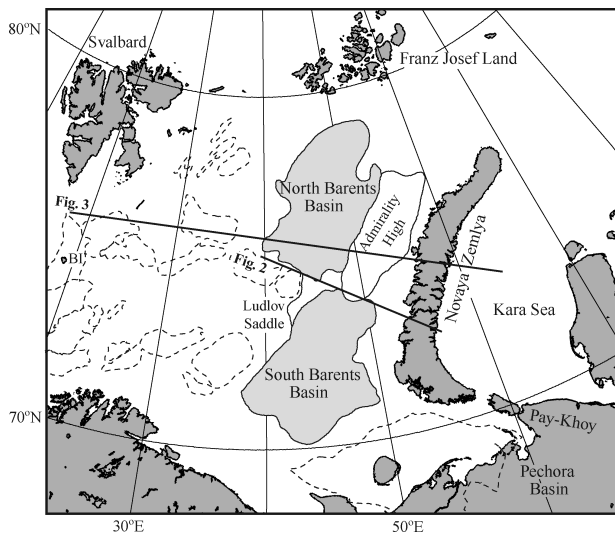


Figure 1. Map showing the location of the basins in the eastern Barents Sea, which are divided in a North and a South Barents Basin. Other basins and highs are stippled. The locations of the sections in Figs 2 and 3 are schematic. BI = Bear Island.

The present-day Barents Sea area consists of a number of basins and highs (Fig. 1), which were formed and deformed by the Timanian (Late Precambrian), Caledonian (Silurian) and Uralian (Permo-Carboniferous) Orogenies and several phases of extension. The Timanian deformation phase is the result of the collision and coalescence of terranes (including Novaya Zemlya and possibly also Franz Josef Land) with the northern margin of Baltica at around 550 Ma. The Caledonian orogeny resulted from the Late Silurian closure of the Iapetus Ocean, which was situated between the Greenland margin of Laurentia and the western margin of Baltica. This event also involved the convergence between Svalbard and the Barents Sea realm (Cocks & Torsvik 2005; Gee 2005). Along the eastern margin of Baltica, the Uralian Ocean had formed by Ordovician and Silurian rifting. Subsequent closure of this ocean in the Late Carboniferous–Early Permian led to continent–continent collision between Kazakhstan and Baltica (forming the Ural Mountains south of Pay-Khoy; Fig. 1) that lasted until the Early Triassic (Brown & Echter 2005).

The origin of the eastern Barents Sea basins is still unclear. The basins are relative deep and have an average sediment thickness of around 13 km (O’Leary *et al.* 2004; Bungum *et al.* 2005). It has previously been assumed that Novaya Zemlya was involved in the Uralian Orogeny and that the basins which lie just west of Novaya Zemlya were foreland basins associated with the Urals (Ziegler 1989). The basins continue southwards into the Timan-Pechora basin, which is probably overprinted along its eastern edge by Permo-Triassic foreland basin subsidence related to the Urals (O’Leary *et al.* 2004). Alternatively, the basins could be the result of multiple phases of extension, which is supported by Permo-Triassic normal faulting and the subsidence histories of the South Barents Sea basin (Johansen *et al.* 1993; Otto & Bailey 1995; O’Leary *et al.* 2004). There is, however, no clear evidence for large-scale normal faulting. O’Leary *et al.* (2004) distinguish three extension episodes in the South Barents basin, based on the determination of subsidence by backstripping and the inversion for strain-rates as a function of time that fit the subsidence profiles: (1) Ordovician–Silurian rifting, associated with the opening of the Uralian Ocean along the eastern margin of Baltica, and subsequent passive margin forma-

tion; (2) Middle-Late Devonian extension with stretching factors between 1.10 and 1.27 and (3) Late Permian–Early Triassic (300–240 Ma) extension with stretching factors >3 and the accumulation of more than 7 km of sediments in the basin centre (see also Otto & Bailey 1995). O’Leary *et al.* (2004) also point out that the similarity in structures and sedimentary thicknesses between the North and South Barents basins suggests similar stretching factors for the Permo-Triassic extension phase for both basins.

The area covered by the Kara Sea on the eastern side of Novaya Zemlya is the offshore continuation of the Siberian Plate (Fig. 1). Similarly to the Barents Sea area, the region consists of highs and basins and its origin is not completely understood. Extension probably occurred in the Permian or Permo-Triassic (Nikishin *et al.* 2002; Vyssotski *et al.* 2006) and was followed by the eruption of the Siberian flood basalts at the Permo-Triassic boundary (around 250 Ma). The Siberian traps further east are a surface expression of this event. The flood basalts could have extended into the Kara Sea and the cooling of the melts may have caused basin subsidence (Vyssotski *et al.* 2006).

Late Triassic inversion structures on the eastern margin of the South Barents basin are shown in the interpretation of a seismic profile in Otto & Bailey (1995) (Fig. 2) (after the report of Baturin *et al.* 1991). The Permian and Triassic rocks are mildly folded, while thrusts are interpreted near the surface at Novaya Zemlya. These thrusts could have been active when the folds were formed, though constraints on the time of formation and activity of the thrusts are difficult to find. Otto & Bailey (1995; see also Torsvik & Andersen 2002) propose that Novaya Zemlya was thrust over the margin of the eastern Barents Sea in the Late Triassic. A contractional event in the eastern Barents Sea is also mentioned by other studies [e.g. Johansen *et al.* 1993; Nikishin *et al.* 2002; Bungum *et al.* 2005 (Fig. 3)], though at different times (between Late Permian and Early Jurassic). The time and magnitude of the compressive movement are thus not well constrained.

In the next section, we first describe the late Palaeozoic to early Mesozoic plate reconstructions for the region and the constraints for the compression phase that can be derived from them. We then present numerical models of shortening of the Barents Sea basin for a generalized 2-D cross-section across the eastern Barents Sea and Novaya Zemlya. The synthesis of the two approaches results in a new plate tectonic scenario for the region.

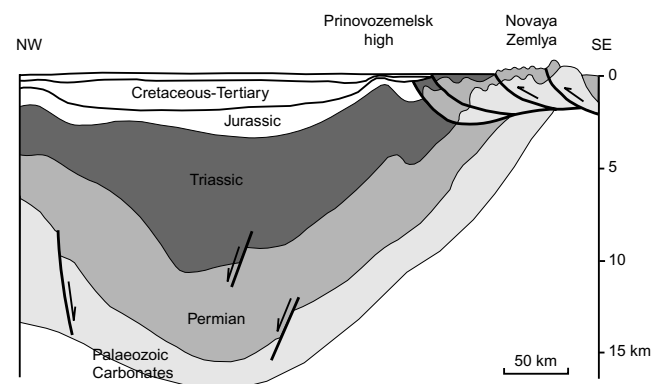


Figure 2. Interpretation of a seismic section through the eastern Barents Sea, showing inversion structures. The section is after Otto & Bailey (1995), the original section is in Baturin *et al.* (1991). We interpret Prinovozemelsk (‘near Novaya Zemlya’) high to be the along-strike continuation of Admiralty High (Fig. 1). Location of section in Fig. 1.

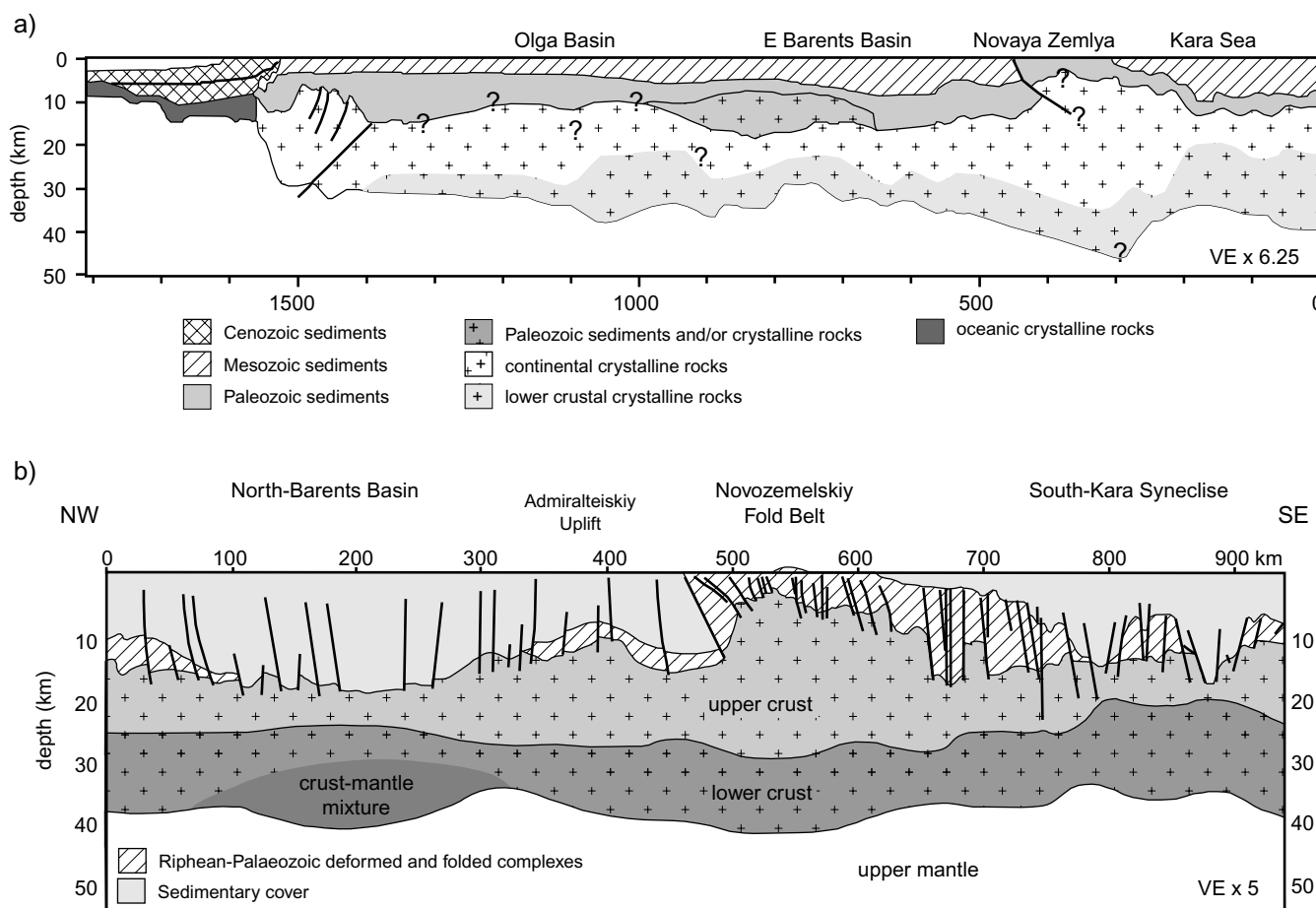


Figure 3. Transects across the eastern Barents Sea and Novaya Zemlya (for location see Fig. 1). (a) After Bungum *et al.* (2005). The interpretation is based on seismological data supplemented with geophysical data. (b) After Ivanova *et al.* (2006). The section is based on multichannel seismic data, wide-angle reflection/refraction profiling and geological/geophysical data.

2 PLATE RECONSTRUCTIONS FOR THE EASTERN BARENTS SEA

The eastern Barents Sea region comprises a number of plates and terranes which were assembled in compressional processes that started in the late Precambrian and probably terminated in the Early Jurassic. Novaya Zemlya forms an integrated part of Baltica since the late Precambrian (coalescence in the Timanian orogeny, Roberts & Olovyanishnikov 2004). At the end of the Carboniferous the Kazakhstan terranes amalgamated with Baltica during the Uralian Orogeny (Fig. 4).

Few methods place reliable constraints upon Palaeozoic–Early Mesozoic plate reconstructions and quantitative reconstructions can only be achieved by using palaeomagnetic methods. There are numerous palaeomagnetic data from Baltica/Stable Europe for the Late Palaeozoic–Early Mesozoic, but unfortunately there are very few reliable palaeomagnetic data from Siberia between the Silurian and the Permo–Triassic boundary. This implies that Siberia's convergence history with the Kazakhstan terranes, Baltica and the independent Kara plate has little quantitative basis and relies heavily on interpolation (Cocks & Torsvik 2007). At around 250 Ma, however, there are many high-quality palaeomagnetic data sets from Siberia. These data are mostly derived from the Siberian Traps (*ca.* 251 Ma; Fig. 4) and differ slightly from Baltica/Stable Europe (Torsvik & Andersen 2002), though the data overlap within error. The differ-

ence allows some post-250 Ma movement of Siberia with respect to Baltica.

The Kara plate includes the North Taimyr and the Severnaya Zemlya archipelago and supposedly collided with Siberia (S–C Taimyr in Fig. 4) during the Late Palaeozoic Uralian Orogeny (Vernikovskiy 1996, 1997). However, the Triassic Taimyr Traps (dated to as young as 227 Ma, Walderhaug *et al.* 2005) experienced younger deformation, indicating that some or all Taimyr deformation occurred in the Late Triassic–Early Jurassic rather than in Uralian times (Inger *et al.* 1999; Torsvik & Andersen 2002). At the same time, Novaya Zemlya may have acted as an allochthonous body that was thrust westward into the eastern Barents Sea. Crustal shortening is also observed in Pay-Khoy (Fig. 1) and mild Triassic–Jurassic inversion is also recognized within the West Siberian Basins (Nikishin *et al.* 2002; Torsvik & Andersen 2002). However, the magnitude of Late Triassic–Early Jurassic movements is difficult to estimate due to lack of high-quality palaeomagnetic data in the region, as well as the resolution power of palaeomagnetic data in general: 1° uncertainty in palaeomagnetic latitude equals 111 km. The Late Permian–Early Triassic reconstructions of Otto & Bailey (1995) and Torsvik & Andersen (2002) imply a subsequent westward movement of Novaya Zemlya of as much as 500–700 km. These estimates derive from the assumption that Novaya Zemlya was aligned with the Ural Mountains and Taimyr in the Uralian and only afterward reached a more westerly position. The displacement estimate seems to be too large, especially since inversion structures

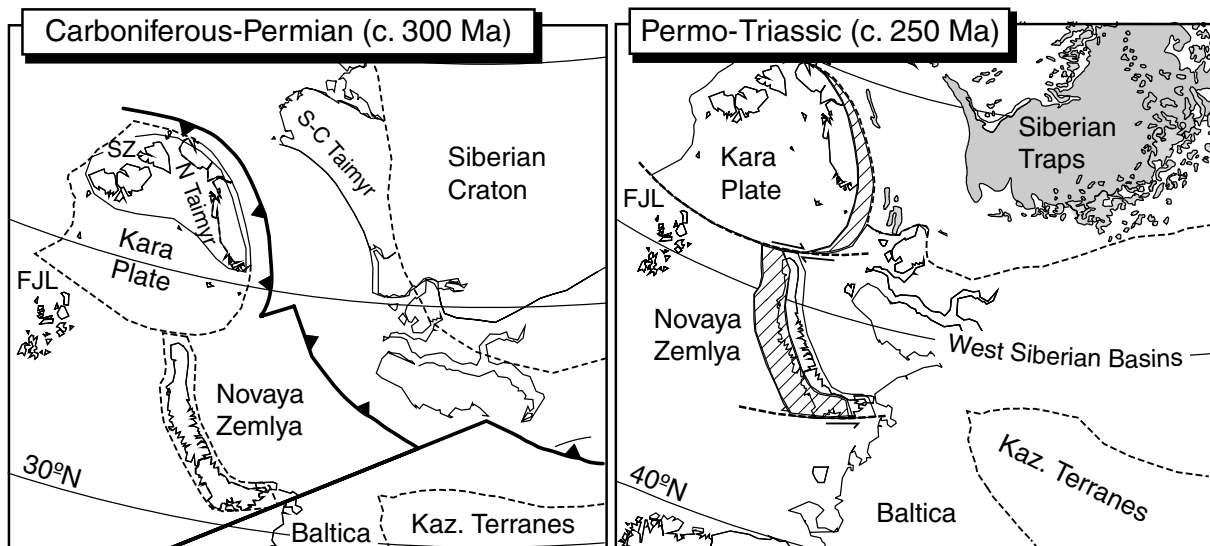


Figure 4. Reconstructions of the eastern Barents Sea realm at around 300 and 250 Ma (modified after Cocks & Torsvik 2007). Striped areas in 250 Ma reconstruction indicate future compressive movements (see text) along the western margin of Novaya Zemlya and the eastern margin of the Kara plate. FJL = Franz Josef Land; SZ = Severnaya Zemlya.

in the East Barents Sea are relatively moderate. Based on preliminary model results of our study, Cocks & Torsvik (2007) reduced this amount considerably and Fig. 4b schematically shows gaps (striped areas) west of Novaya Zemlya and along the Taimyr margin that are considered to be compressed by subsequent Late Triassic–Early Jurassic deformation.

Since no independent data can constrain the actual amount of westward movement of Novaya Zemlya, we here try to resolve this issue by combining plate reconstructions with numerical models which are aimed at investigating the amount of shortening that would agree with the mild level of inversion structures observed in the eastern Barents Sea. We suggest that deformation in the eastern Barents Sea could be the result of continued movement of the Siberian plate in the Late Triassic–Early Jurassic, which is perhaps driven by far-field stresses related to the destruction of the Palaeotethys (Kimmerian tectonic phase). The convergence direction is approximately perpendicular to the strike of Novaya Zemlya. We first consider a modest scenario in which 300 km convergence occurred over a 30 Myr interval, that is, between 220 and 190 Ma. This is also the time period where we invoke sinistral strike slip deformation along the western Barents Sea margin using a new model developed by Torsvik *et al.* (2006). This strike-slip deformation probably resulted from intra-Pangean rifting between Baltica and Laurentia, with Laurentia (including Greenland) rotating clockwise relative to Baltica.

3 NUMERICAL MODELS OF BASIN INVERSION

3.1 Modelling approach

We attempt to better constrain the magnitude of shortening associated with inversion in the eastern Barents Sea by combining numerical models of basin inversion with plate reconstructions. Our approach will result in an order-of-magnitude estimate of the shortening (i.e. tens versus hundreds of kilometres). Further refinement will at present not be feasible due to uncertainties associated with the choice of the initial geometry and the rheology, which are poorly

constrained by the available data, and a difficult to estimate uncertainty inherently caused by the representation of the complexity of a natural setting in a simplified model experiment. We will investigate the sensitivity of our model to variations in rheology and geometry.

Basin inversion has been investigated with many analogue (e.g. Buchanan & McClay 1991; Eisenstadt & Withjack 1995; McClay 1995; Brun & Nalpas 1996; Panien *et al.* 2005; Del Ventisette *et al.* 2006) and fewer numerical (Hansen *et al.* 2000; Buiter & Pfiffner 2003; Hansen & Nielsen 2003) models. We use a numerical approach because this allows the application of a temperature-dependent rheology and gives large freedom in investigating the effects of variations in material properties and model setup. The equation of mechanical equilibrium for incompressible flows and the heat equation are solved using an arbitrary Lagrangian–Eulerian formulation. The code (Sopale) is 2-D plane-strain and is characterized by its ability to achieve large deformations with free surface behaviour (Fullsack 1995). The modelling method has been shown to well reproduce results of laboratory models of shortening and inversion in granular materials (Buiter *et al.* 2006; Panien *et al.* 2006).

The model materials deform according to a viscous-plastic rheology (Table 1). Frictional-plastic behaviour is modelled by an incompressible Drucker–Prager frictional criterion:

$$(J_2')^{1/2} = P(1 - \lambda) \sin(\phi) + C \cos(\phi), \quad (1)$$

where J_2' is the second invariant of the deviatoric stress tensor, P dynamic pressure, λ pore fluid factor, ϕ angle of internal friction and C cohesion. We use a relatively standard value of 30° for the crustal value of ϕ (following high pressure data of Byerlee 1978). The pore fluid factor is hydrostatic and effectively reduces the brittle material strength ($\phi = 30^\circ$ for $\lambda = 0.36$ is similar to $\phi = 19^\circ$ for $\lambda = 0$) (Beaumont *et al.* 1996). We assume that frictional materials weaken with strain. This strain softening is simulated by a simple linear decrease of the angle of internal friction with increasing strain [which is measured as accumulated effective deviatoric strain, $(\frac{1}{2} \epsilon_{ij} \epsilon_{ij})^{1/2}$]. Bos & Spiers (2002) suggest that weakening by pressure solution-controlled flow of fine-grained fault

Table 1. Model material properties.

Material property	Sedi	Crust	Strong
Angle internal friction ϕ	15°	30°	50°
Cohesion C (MPa)	10	10	100
Pore fluid factor λ (hydrostatic)	0.42	0.36	0.36
Density (kg m ⁻³)	2400	2800	2800
Wet quartzite ^a :			
Power-law const. A^b (s ⁻¹ Pa ⁻ⁿ)		8.574×10^{-28}	
Power-law exponent n		4.0	
Power-law act.energy Q (kJ mole ⁻¹)		223	
scaling factor c	1	1	2
Wet anorthite ^c :			
Power-law const. A^b (s ⁻¹ Pa ⁻ⁿ)		1.8×10^{-15}	
Power-law exponent n		3.0	
Power-law act.energy Q (kJ mole ⁻¹)		356	
scaling factor c	1	1	2
Thermal diffusivity (m ² s ⁻¹)		10^{-6}	
Thermal expansion (K ⁻¹)		0	
Heat production (W m ⁻³)		9×10^{-7}	

^aGleason & Tullis (1995).^bModified to a general state of stress (Ranalli 1987).^cRybacki & Dresen (2000).

rock may be included in geodynamic models by a decrease in apparent friction coefficient from ~ 0.75 for unstrained material to ~ 0.3 for highly strained material. We keep approximately the same ratio and reduce the angle of internal friction to half of its value ($\phi \rightarrow \phi/2$) over a strain interval of 0.5–1.5. Viscous deformation follows either linear-viscous behaviour [$(J_2')^{1/2} = 2\eta\dot{\epsilon}_2$] or power-law creep:

$$(J_2')^{1/2} = cA^{-1/n}\dot{\epsilon}_2^{1/n}e^{Q/nRT}, \quad (2)$$

where η is viscosity, A a constant, n power-law exponent, $\dot{\epsilon}_2$ second invariant of the strain-rate tensor, Q thermal activation energy, R gas constant, T temperature and c a scaling factor (usually 1). We test two flow laws: a wet quartzite flow law (Gleason & Tullis 1995), which results in a relatively weak lower crust in comparison with the strength profiles from other flow laws, and a strong flow law for wet anorthite (Rybacki & Dresen 2000) (Fig. 5). Alternatively, we could have varied the strength of the lower crust by varying the temperature or strain-rate. The results of the weak (strong) flow law can to first order be interpreted as representing a warm, slow-deforming (cold, fast-deforming) environment.

At the surface of the models, material is removed or added following simple erosion and sedimentation laws. For diffusive erosion and sedimentation, the rate of topography change depends on surface curvature (Culling 1960):

$$\frac{dh}{dt} = \kappa \frac{d^2h}{dx^2}, \quad (3)$$

where h is the topography and κ the diffusion coefficient. For slope-dependent erosion the topography change follows:

$$\frac{dh}{dt} = k \frac{dh}{dx}, \quad (4)$$

where k is an erosion coefficient. These are simplified representations of the complex surface processes in nature. We have chosen to test different surface processes models, because not much is known about the erosion and sedimentation history of the eastern Barents Sea in the Late Triassic–Early Jurassic.

Extensional sedimentary basins may form structural weaknesses in the lithosphere where shortening preferentially localizes even after the thermal signature of extension should have been dissipated

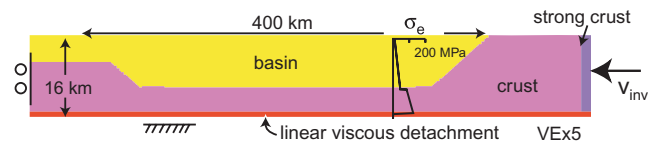
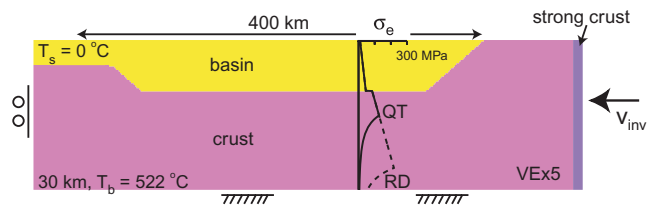
a) rigid-plastic model**b) viscous-plastic model**

Figure 5. Setup and boundary conditions for the numerical models. (a) Rigid-plastic model (23 040 Eulerian elements and minimum 208 633 Lagrangian tracking points). (b) Thermo-mechanical model (32 400 Eulerian elements and minimum 292 951 Lagrangian tracking points). GT = flowlaw for wet quartzite of Gleason & Tullis (1995); RD = flowlaw for wet anorthite of Rybacki & Dresen (2000). The flowlaws are plotted for a lithostatic pressure and a strain-rate of 10^{-15} s⁻¹.

away. Previous studies have pointed out that this weakening may be related to the replacement of competent crustal rocks by weaker sediments during basin formation, thermal blanketing by low conductivity sediments (and associated weakening due to higher temperatures) and the presence of normal faults that can be re-used in compression (Ziegler *et al.* 1995; Sandiford 1999; Hansen & Nielsen 2003). We, therefore, consider a basin which is filled with sediments which are weaker than the surrounding crust (Table 1). By starting from a pre-defined basin (Fig. 5), we avoid modelling the uncertain formation history of the basin. The available geological and seismic data indicate that large-scale normal faults are absent in the basin area and we have, therefore, not included pre-existing normal faults.

Our 2-D model follows a simplified and generalized section across Novaya Zemlya and the eastern Barents Sea basins. From the data presented in Ivanova *et al.* (2006), Bungum *et al.* (2005) and Ritzmann *et al.* (2007) (Fig. 3) we infer that the width of the eastern Barents Sea basins is at present around 400 km and that the crustal thickness underneath them is approximately 20 km. We assume that these values are more or less representative for the situation at the end of basin formation. This is valid as long as the shortening event was of limited magnitude, which is supported by the mild inversion structures observed in the basin and by our modelling results. Our model basin is 10 km deep. We include a 5 km thick sediment layer to the west of the basin, to account for a sediment cover in the central Barents Sea. Not much is known on the cause of the compressional deformation of the basins. We speculate that inversion in the eastern Barents Sea was caused by westward movement of the Siberian plate. Deformation in our models is, therefore, driven by a westward velocity at the Siberian plate margin. To avoid localization of deformation in the Siberian plate, we first model the Siberian plate itself as a strong block (Table 1) indenting Novaya Zemlya. This block only provides the driving velocity and has no real physical meaning in our models. We later test the effect of this assumption by adopting a standard crustal strength for the Kara Sea area.

The models with a temperature-dependent rheology have a surface temperature of 0 °C and a Moho temperature (at 30 km) of 522 °C. This initially corresponds to a surface heat flow of 57 mW m⁻². This is within the range of the sparse heat flow data

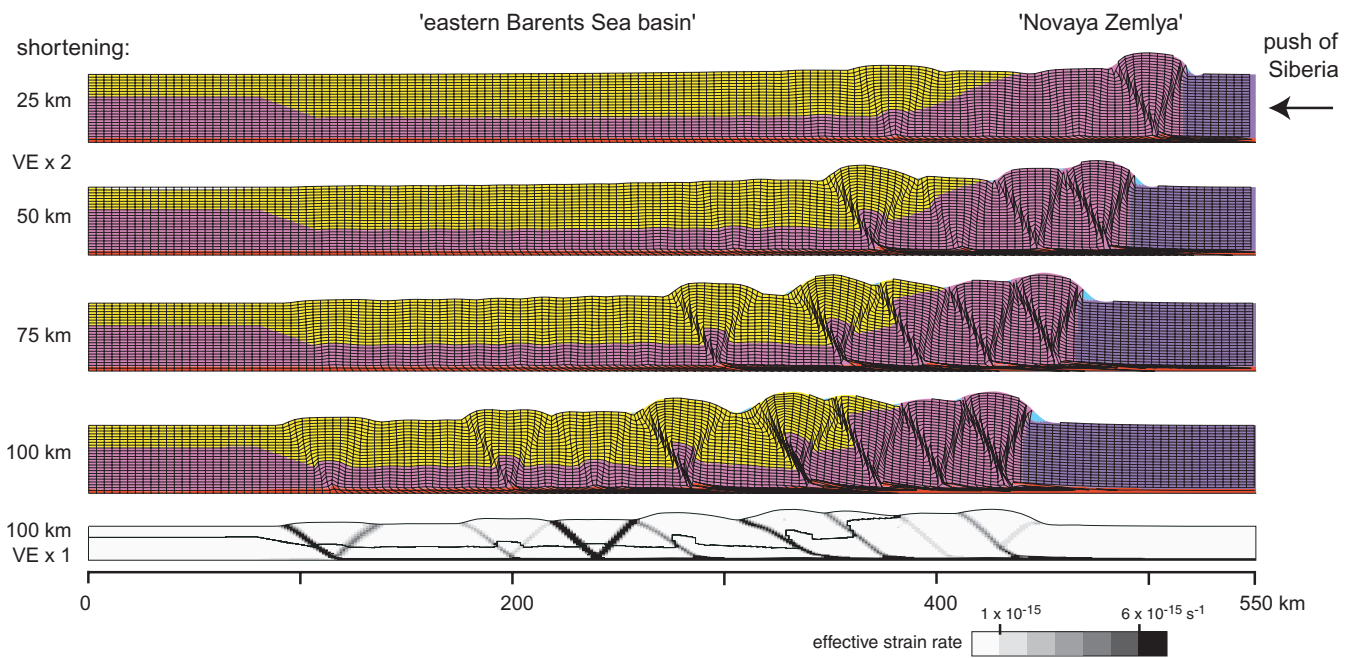


Figure 6. Evolution of reference model 1. The total amount of shortening is indicated at the left-hand side of the models. Shear-zones and fault-bend-folds develop in the frictional-plastic basin sediments and underlying crust due to the basinward movement of a strong crustal block over a linear-viscous detachment (viscosity 10^{20} Pa s). The grid is a Lagrangian tracking grid of which every 8th line in the horizontal and vertical direction is shown. The model setup is shown in Fig. 5a. Vertical exaggeration is 2 (except for bottom figure).

in the south of the Barents Sea (not above salt diapirs) and the Kara Sea (Artemieva & Mooney 2001; Bugge *et al.* 2002).

In the next section, we first describe a simple inversion model on the scale of the upper crust (Fig. 5a). In this model, the lower crust is represented by a thin linear-viscous basal detachment. We then test the effects of (1) basal detachment strength, (2) surface processes, (3) pre-existing thrusts, (4) the presence of a lower crust and its strength (Fig. 5b) and (5) the strength of the Kara Sea domain. We aim to find an upper limit to the amount of displacement associated with the movement of the Siberian plate by searching for a simple model that reproduces the main characteristics of the eastern Barents Sea basin inversion: localization of shortening near the eastern basin margin and mild folds in the basin fill.

3.2 Brittle inversion models

3.2.1 Model 1

In our first models the sediments and crustal materials are temperature-independent rigid-plastic. The combined thickness of upper crust and basin is 15 km and the models are underlain by a 1 km thick linear-viscous detachment (Fig. 5a). This detachment can be viewed as a pre-existing horizontal detachment fault or as a very simple representation of viscous lower crust behaviour. We use a shortening velocity of 1 cm yr^{-1} . However, because most materials in this model (sediments and upper crust) are rigid-plastic, their behaviour is not velocity-sensitive. The velocity dependence of the linear-viscous basal detachment is investigated by varying its viscosity (see next Section 3.2.2). The detachment in Model 1 has a viscosity of 10^{20} Pa s. At the surface a minor amount of diffusive erosion and sedimentation is applied with a coefficient of $5 \times 10^{-8} \text{ m}^2 \text{ s}^{-1}$ (Table 2).

The results in Fig. 6 show that deformation first localizes at the right-hand side of the model by forming shear-zones and pop-ups in

the Novaya Zemlya domain and at the eastern (right-hand) side of the basin. Deformation propagates through the model and has reached the far side of the basin after around 75 km of shortening. Both basin fill and the underlying upper crust are involved in shear-zone formation and associated folding. The base of the model below the linear-viscous detachment is held fixed. This basal boundary condition simulates a setting where the upper crust is coupled to the lower crust and thus restricted in horizontal displacements at its base. The strength and thickness of the basal detachment layer determine how fast deformation propagates from the right (or east) side of the model where the velocity is applied to the left (or west). This is investigated further in Sections 3.2.2 and 3.3. The style of deformation in this model resembles models of the formation of fold-and-thrust belts (e.g. Mulugeta 1988; Storti *et al.* 2000; Schreurs *et al.* 2001), where shortening is accommodated by the formation of forward thrusts and backthrusts, which form more or less in-sequence towards the foreland. The in-sequence behaviour is partly disrupted in our model because of the preferred localization of shortening in the weaker sediments of the basin. The model indicates that a limited amount of displacement of the Siberian plate leads to deformation of the entire basin. This does not correspond to observations that indicate that deformation is more restricted to the eastern part of the basin. The model, therefore, provides an upper limit to the displacement of the Siberian plate (Table 2). Fast propagation of deformation through the basin area is facilitated by the basin fill being weaker than the crust and by the linear-viscous basal detachment.

3.2.2 Influence of basal detachment strength (models 2–4)

A higher value for the viscosity of the detachment (viscosity = 2×10^{20} Pa s) focuses deformation to the right-hand side of the model and in some cases even initiates deformation of the strong crustal block (model 2, Fig. 7a). Because the detachment is linear

Table 2. List of models.

Model	Rheol. ^a	Basal detachm.		Surface processes ^b	Max. short. ^c (km)	Remark	Figures
		Thick (km)	Visc (Pa s)				
1	RP	1	10^{20}	$d\ 5 \times 10^{-8}\ \text{m}^2\ \text{s}^{-1}$	75	Reference model	6
2	RP	1	2×10^{20}	$d\ 5 \times 10^{-8}\ \text{m}^2\ \text{s}^{-1}$	125		7a
3	RP	1	5×10^{19}	$d\ 5 \times 10^{-8}\ \text{m}^2\ \text{s}^{-1}$	50		7c
4	RP	1	10^{20}	$d\ 5 \times 10^{-8}\ \text{m}^2\ \text{s}^{-1}$	25	Decoupled at base	7d
5	RP	1	10^{20}	$d\ 2 \times 10^{-6}\ \text{m}^2\ \text{s}^{-1}$	100		8b
6	RP	1	10^{20}	sl $9.5 \times 10^{-11}\ \text{m}\ \text{s}^{-1}$	100		8c
7	RP	1	10^{20}	total	> 200		8d
8	RP	1	10^{20}	$d\ 5 \times 10^{-8}\ \text{m}^2\ \text{s}^{-1}$	75	Pre-exist thrusts $10^{20}\ \text{Pa}\ \text{s}$	9
9	RP	3	10^{20}	$d\ 5 \times 10^{-8}\ \text{m}^2\ \text{s}^{-1}$	50		10b
10	RP	5	10^{20}	$d\ 5 \times 10^{-8}\ \text{m}^2\ \text{s}^{-1}$	25		10c
11	RP	15	10^{20}	$d\ 5 \times 10^{-8}\ \text{m}^2\ \text{s}^{-1}$	25		10d
12	VP	–	–	$d\ 5 \times 10^{-8}\ \text{m}^2\ \text{s}^{-1}$	75	Gleason & Tullis (1995)	11a
13	VP	–	–	$d\ 5 \times 10^{-8}\ \text{m}^2\ \text{s}^{-1}$	175	Rybacki & Dresen (2000)	11b
14	RP	1	10^{20}	$d\ 5 \times 10^{-8}\ \text{m}^2\ \text{s}^{-1}$	75	no strong SIB	12a
15	VP	–	–	$d\ 5 \times 10^{-8}\ \text{m}^2\ \text{s}^{-1}$	50	GT, no strong SIB	12b

^aRP = rigid-plastic rheology, VP = viscous-plastic rheology (Fig. 5).

^bd = diffusive erosion and sedimentation, sl = slope-dependent erosion.

^cAn indication of the upper limit of Siberian plate displacement is determined by the shortening at which the deformation reaches the west basin margin.

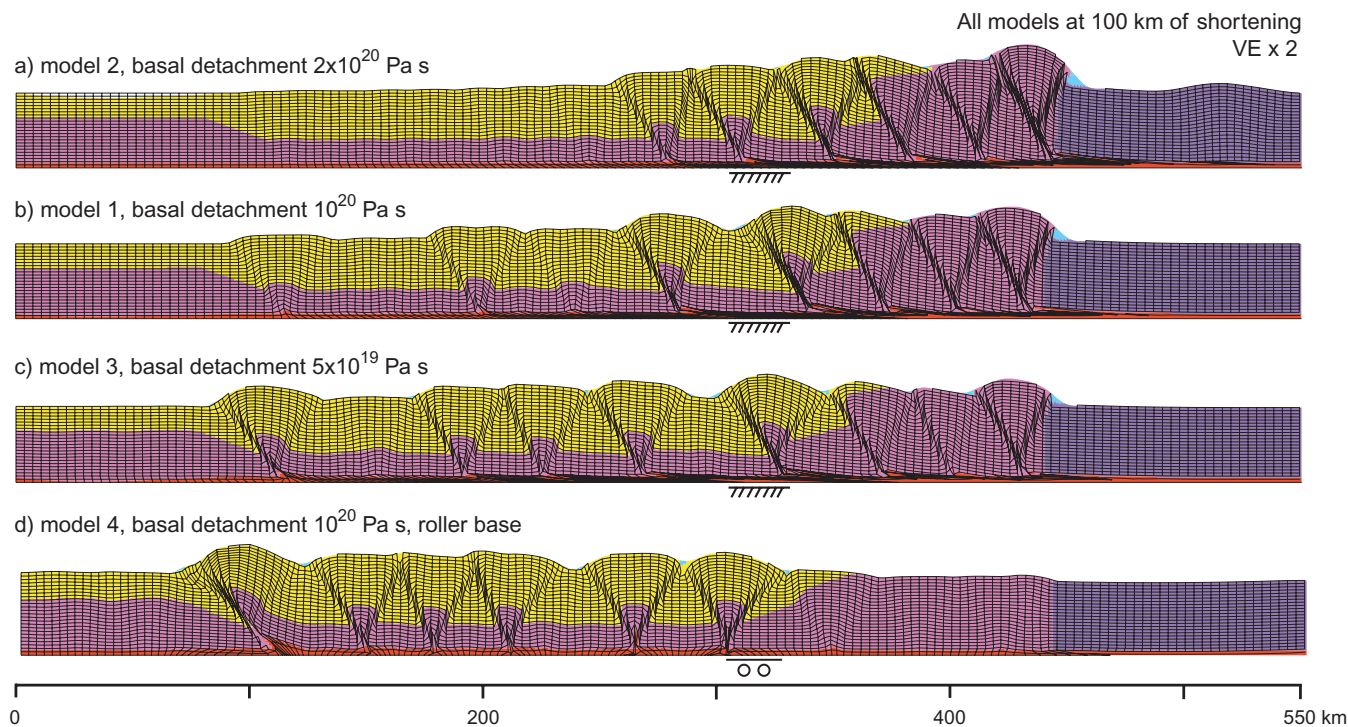


Figure 7. The propagation of deformation through the models is to a large degree influenced by the level of decoupling at the base of the upper crust. (a–c) Models 1–3 illustrate the sensitivity to the viscosity value of the basal detachment. (d) Model 4 with a roller basal boundary condition (free horizontal movement) shows efficient transfer of shortening through the basin. The models are shown at 100 km of shortening. Vertical exaggeration is 2.

viscous and the overlying materials are brittle and, therefore, velocity-independent, a higher viscosity value for the basal detachment is equivalent to using a higher velocity (i.e. $1\ \text{cm}\ \text{yr}^{-1}$ and $2 \times 10^{20}\ \text{Pa}\ \text{s}$ is equivalent to $2\ \text{cm}\ \text{yr}^{-1}$ and $10^{20}\ \text{Pa}\ \text{s}$). A weaker basal detachment (viscosity = $5 \times 10^{19}\ \text{Pa}\ \text{s}$, model 3, Fig. 7c) transfers deformation efficiently through the basin and already after 50 km of shortening thrusting is initiated at the left-hand side of the basin (Table 2). In this case, the weak material of the detachment layer effectively decouples the overlying brittle crust from the base of the model. The most effective decoupling is obtained

when horizontal movement at the base is unrestricted (roller boundary condition) as in model 4 (Fig. 7d). In this case, the entire basin is uplifted and thrusts form at both basin margins already in early stages of the shortening. As the effects of shortening in the eastern Barents Sea are restricted to the eastern part of the basins it is considered likely that the lower crust in this area possesses a strength which is high enough to restrict horizontal movements of the upper crust above it. We therefore, consider models with a basal detachment which is not too weak and a fixed horizontal base.

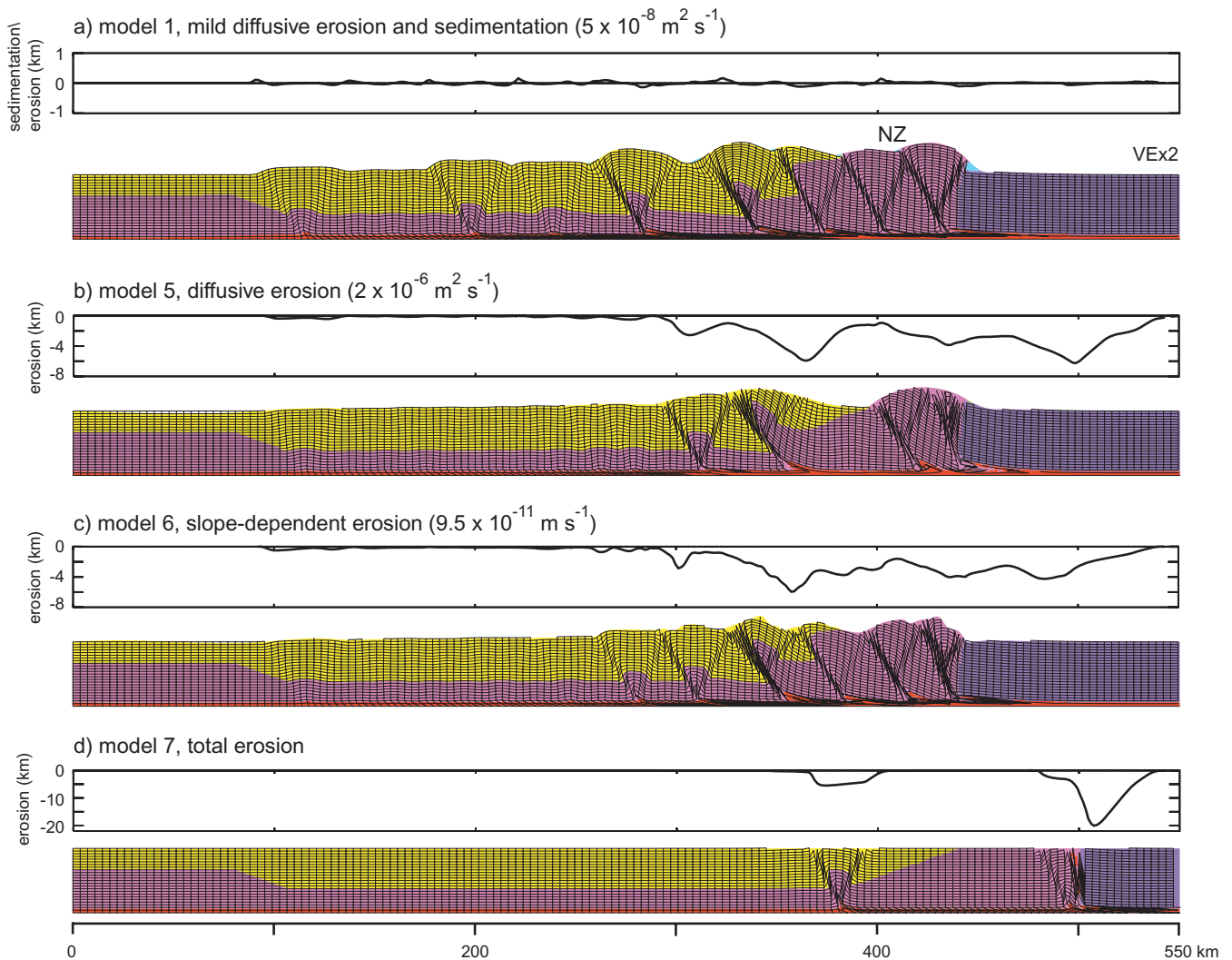


Figure 8. Influence of surface processes on the localization of shortening. The panels above each model show the amount of eroded (models 5–7) or eroded and sedimented (model 1) material. Erosion and sedimentation is measured at fixed points in space (Eulerian reference frame). Note the different scale on the erosion panels. The models are shown at 100 km of shortening with a vertical exaggeration of 2. NZ = model equivalent of Novaya Zemlya.

3.2.3 Influence of surface processes (models 5–7)

The previous models (1–4) have an almost negligible amount of erosion and sedimentation at their surface. However, surface processes have been shown to influence compressional tectonic processes (Koons 1990; Beaumont *et al.* 1992; Willett 1999; Simpson 2006; Pysklywec 2006, among others) and they could influence the effectiveness of localization of shortening in our model basin. We examine the model response to (1) diffusive erosion, (2) slope-dependent erosion and (3) total erosion. Diffusive erosion (with a coefficient of $2 \times 10^{-6} \text{ m}^2 \text{ s}^{-1}$, no sedimentation) leads to focusing of deformation to the right part of the model (model 5, Fig. 8b). Deformation has still reached the far side of the basin by 100 km of shortening, but in a less pronounced manner than in the reference model (model 1 in Fig. 8a). Slope-dependent erosion with a coefficient of $9.5 \times 10^{-11} \text{ m s}^{-1}$ leads to a similar style of behaviour (model 6, Fig. 8c). The erosion coefficients for these two models have been chosen such that similar amounts have been eroded at 100 km of shortening. The extreme case is total erosion, where all material above the initial model surface is removed during model evolution (model 7, Fig. 8d). In this model most shortening is lo-

calized at the transition between the strong block ('Siberia') and the normal crust ('Novaya Zemlya'), though some thrusting still occurs at the eastern edge of the basin.

Removal of the overburden by erosion leads to local relative weakening in frictional materials due to the reduction in the lithostatic component of the pressure (eq. 1), facilitating continued uplift along thrust ramps. Conversely, sedimentation tends to suppress deformation through the strengthening effect of an increased overburden (see also Simpson 2006). An alternative approach to understanding the effects of surface processes on our models is to compare them to critical thrust wedges (Dahlen 1984). Erosion in our models is mainly concentrated on material uplifted along the thrusts towards the rear of the model (where local surface curvature and surface slope are highest) and causes a reduction of the surface slope. This leads to a subcritical value for the taper angle of the model wedge and the model reacts by internal deformation to recover the critical taper value (e.g. Dahlen & Barr 1989). Deformation will thus be concentrated in areas where material has been removed by erosion. These models show that surface erosion helps to localize shortening to the eastern part of the model and that thrusts in that domain tend to have larger offsets. The existing information on the

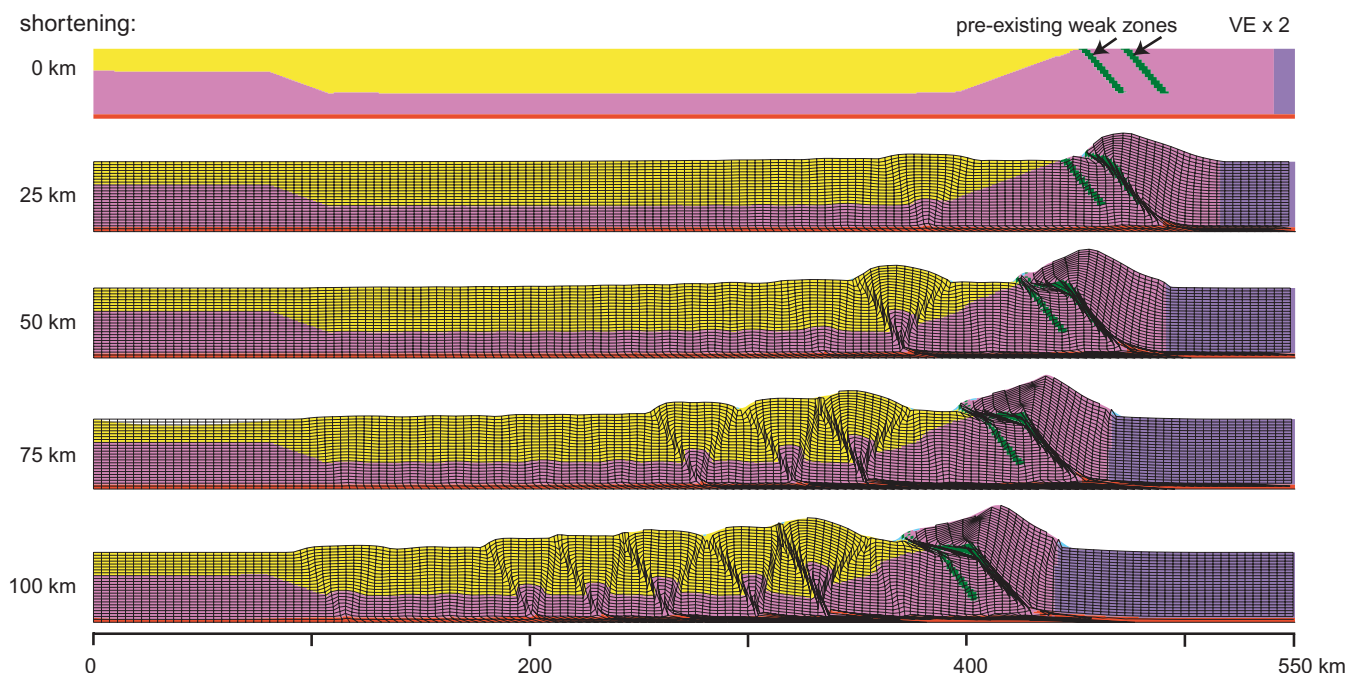


Figure 9. Influence of pre-existing thrusts in the upper crust (simulating older thrusts at Novaya Zemlya) (model 8). Vertical exaggeration is 2.

level of erosion at Novaya Zemlya and in the eastern Barents Sea in the Late Triassic to Early Jurassic is unfortunately rather scarce. Johansen *et al.* (1993) report an erosional unconformity in the North and South Barents Basin at the Triassic–Jurassic boundary which may speculatively be related to the compressional episode we are studying here. Our models indicate that with reasonable levels of erosion (e.g. Figs 8b and c) deformation still reaches the west side of the basin after around 100 km of shortening. This provides again an upper bound to the displacement associated with the shortening event (Table 2).

3.2.4 Influence of pre-existing shear zones (model 8)

Most of the previous models indicate that the westward movement of the indenter ('Siberia') could easily have led to substantial thrusting in the sedimentary basin, with deformation of both sediments and the upper crust. Some of the shortening is accommodated at the crustal block representing Novaya Zemlya. Novaya Zemlya was affected by orogenies before the Late Triassic–Early Jurassic, such as the Timanian and possibly the Uralian Orogeny (with peak deformation at 290–300 Ma). These would have led to the formation of thrusts, which may have been re-used in the later compression caused by the movement of the Siberian plate. We, therefore, here investigate the sensitivity of our models to pre-existing weak shear zones in the 'Novaya Zemlya' block (model 8, Fig. 9). The aim of this model is to investigate whether displacement along pre-existing thrusts could have reduced the level of deformation in the eastern Barents Sea basins. We are not reproducing existing thrusts at Novaya Zemlya, but instead include two weak zones with a 30° dip angle. The pre-existing thrusts are simulated as strips of three elements wide with a linear-viscous rheology (viscosity 10^{20} Pa s) (*cf.* Buiter & Pfiffner 2003). This is a simple manner to simulate a weak region and is not meant to imply that shear zones would behave in a linear-viscous manner. Fig. 9 shows that the right-most pre-existing shear zone is activated early in model evolution. The upper crustal layer climbs

up along the thrust ramp and is thrust over the margin of the basin, approaching the thin-skinned nature of the deformation interpreted in Fig. 2. The deformation in the basin resembles the model without pre-existing shear zones (model 1, Fig. 6) and shear zones form at the far end of the basin before 100 km of shortening. This may indicate that the pre-existing shear zones in the 'Novaya Zemlya' block do not influence the thrusting in the basin to a large degree.

3.3 Brittle-viscous inversion models (models 9–13)

The models in the previous sections consist of brittle sediments and upper crust, underlain by a weak linear-viscous detachment of 1 km thick. To investigate the influence of the lower crust on the localization of shortening in the upper crust, we first stepwise increase the thickness of the linear-viscous layer until it extends to the base of the crust at 30 km. A thicker viscous layer will reduce the impact of the boundary conditions at the bottom of the model. This is important in two aspects: (1) A thick basal layer may facilitate horizontal movements at the base of the upper crust. Model 4 (Fig. 7d) already illustrated that free movement at the base of the upper crust (roller) promotes fast propagation of deformation across the model domain and early inversion of the basin. (2) A thick viscous layer may allow vertical movements at the base of the upper crust. This effectively implements a simple form of isostatic compensation. Models 9–11 (Fig. 10) show that a thicker viscous layer transfers shortening efficiently along the entire basin. Fewer thrusts form in the Novaya Zemlya block and in the basin area itself, until shortening is mainly localized along shear zones at each side of the basin (Fig. 10d). The upper crust is underthrust along these shear zones. The uplift of the basin and thrusting at the basin sides resembles a more 'classic' style of basin inversion (Cooper *et al.* 1989).

Temperature-dependent creep in the lower crust leads to a different strength profile than in the case of linear-viscous flow. It is characterized by a high strength at the brittle-viscous transition,

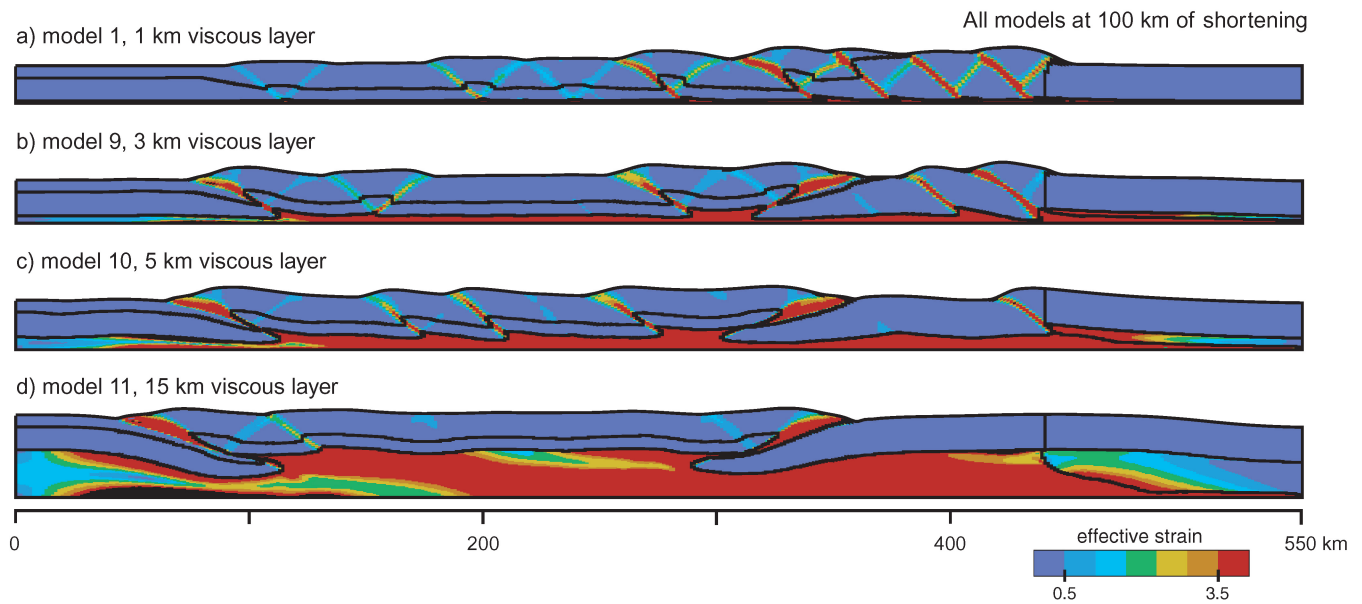


Figure 10. Illustrates the influence of increasing thickness of a linear viscous lower layer with viscosity 10^{20} Pa s on the localization of shortening in the brittle upper layer (with a fixed thickness of 15 km). Strong linear viscous lower crust (indenter at the right-hand side of the model) has a viscosity of 10^{21} Pa s and a 1 km thick basal detachment of 10^{20} Pa s, while its strong brittle upper crust is identical to the strong crustal block in models 1–8 (Table 1). All models are at 100 km shortening and have no vertical exaggeration.

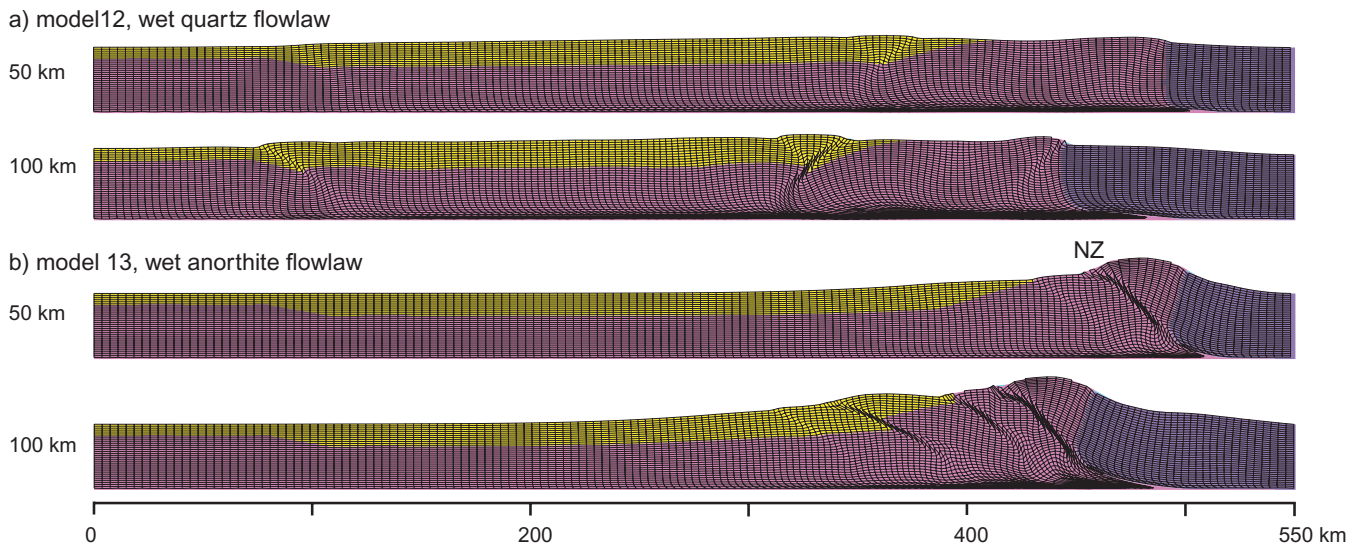


Figure 11. Evolution of viscous-plastic models with temperature-dependent creep (model set-up in Fig. 5b). (a) Model 12 with flowlaw of Gleason & Tullis (1995). Distributed uplift of the basin area is visible after 50 km of shortening, while shear zones have formed at the basin sides after 100 km of shortening. (b) Model 13 with flowlaw of Rybacki & Dresen (2000). The stronger flowlaw leads to localization of shortening at the right-hand side of the model, with the formation of shear zones in the Novaya Zemlya (NZ) domain and in the eastern part of the basin.

which decreases downwards (Fig. 5b). Horizontal movements at the base of the upper crust could, therefore, be more restricted in models with creep flow. The transition between brittle and viscous material behaviour in the creep models is determined by the values for temperature, strain-rate and pressure and the parameters in the plasticity and creep laws (eqs 1 and 2). In model 12 we have used the relatively weak flowlaw for wet quartzite (Gleason & Tullis 1995, Table 1, Fig. 5b). The entire basin is inverted (Fig. 11a) with uplift of the basin sediments after 50 km of shortening and the formation of thrusts at both basin sides by 100 km of shortening. The

inversion style has similarities to the model with a thick linear viscous lower crust (model 11, Fig. 10). In these models, shortening leads to efficient propagation of deformation throughout the basin. The available data (though sparse) seem however to indicate that deformation is more limited to Novaya Zemlya and the east side of the basins. This could imply that only a low amount of shortening occurred and/or that the lower crust is stronger. A model with a stronger flowlaw [model 13 with wet anorthite of Rybacki & Dresen (2000), Figs 5b and 11b] leads indeed to focusing of deformation in the Novaya Zemlya domain and at the eastern side of the basin. In

these domains thrusts form that dip towards the indenting Siberian plate.

3.4 The role of the Siberian plate (models 14–15)

In our models we have assumed that shortening was caused by displacement of the Siberian plate. Within data resolution power, palaeomagnetic data for Siberia and Baltica (inset in Fig. 13, see also Cocks & Torsvik 2007) allow post-Permian relative movements of more than 1000 km. Our models show that substantial deformation of the eastern Barents Sea basins and Novaya Zemlya already occurs for far smaller displacement magnitudes. The indentation in the Novaya Zemlya region is consistent with models in which Siberia and Baltica/Kazakhstan converged in a large-scale sinistral transpressional system (Natal'in *et al.* 2005; Van der Voo *et al.* 2006).

The western part of the Siberian 'indenter' is occupied by the Kara Sea (Fig. 1), directly to the east of Novaya Zemlya. Extension in the Kara Sea is likely to have taken place in the Late Permian to Mid Triassic (Nikishin *et al.* 2002; Vyssotski *et al.* 2006) and could have weakened the Siberian plate margin. In such a scenario, the westward displacement of Siberia may be expected to have caused shortening not only in Novaya Zemlya and the basins to its west, but likely also in the Kara Sea. We have tested two models in which the Siberian domain is not simulated as a strong indenter, but instead as crust with the same properties as the crust of the Novaya Zemlya domain and the crust underlying the eastern Barents Sea basins (models 14 and 15, Fig. 12). In the rigid-plastic case (model 14), thrusts now also form in the western Siberian domain, taking up part of the shortening. The viscous-plastic case (model 15) shows more distributed deformation in the domain of the Siberian indenter in comparison with the case of a strong indenter (model 12). Shear zone formation in the eastern Barents Sea model area is less pronounced than in the corresponding models with strong indenter, but still of substantial level. Deformation involves the entire basin at slightly less amounts of shortening for the cases without strong indenter (Table 2). A weak Siberian plate margin could thus have ac-

commodated part of the shortening associated with the convergence of Siberia and Baltica at Novaya Zemlya. Mild Triassic–Jurassic inversion is recognized in the West Siberian Basin to the east of the Kara Sea (Torsvik & Andersen 2002), but we have not found indications for contemporaneous inversion in the Kara Sea. This seems to indicate that the Siberian plate indeed moved as a relatively rigid block. We can, however, not completely rule out minor inversion in the Kara Sea and we will allow for this uncertainty in our estimate of Siberia's displacement.

The available data seem to indicate that inversion structures in the eastern Barents Sea basins are relatively minor and that thrusts at Novaya Zemlya could have accommodated large offsets. It is unknown whether the thrusting is an indication of deformation which occurs at shallow levels only (upper few kilometres to upper crust), or whether deformation occurs throughout the crust and lithosphere, but in a more distributed manner. We expect that part of the westward movement of Siberia would have been taken up by the Novaya Zemlya thrusts, which is also supported by our models.

4 SYNTHESIS: A NEW PLATE RECONSTRUCTION

The eastern Barents Sea basins experienced mild inversion as the Siberian plate margin was pushed into Novaya Zemlya in the Late Triassic–Early Jurassic. Keeping in mind all shortcomings associated with representing a natural situation in a numerical model, our models indicate that shortening would have deformed the eastern Barents Sea basins already in early stages of the convergence and that deformation could in most cases have involved the entire basin by 100 km of shortening (Table 2). Localization of deformation in the eastern part of the basin and at Novaya Zemlya is promoted by (1) a high strength of the lower crust, through either a high viscosity detachment (Fig. 7) or a strong creep law (Fig. 11), (2) surface erosion (Fig. 8) and/or (3) small amounts of shortening (Fig. 6). Novaya Zemlya may have been pushed westward in a thin-skinned manner (as seems to be indicated on the interpreted section of Otto

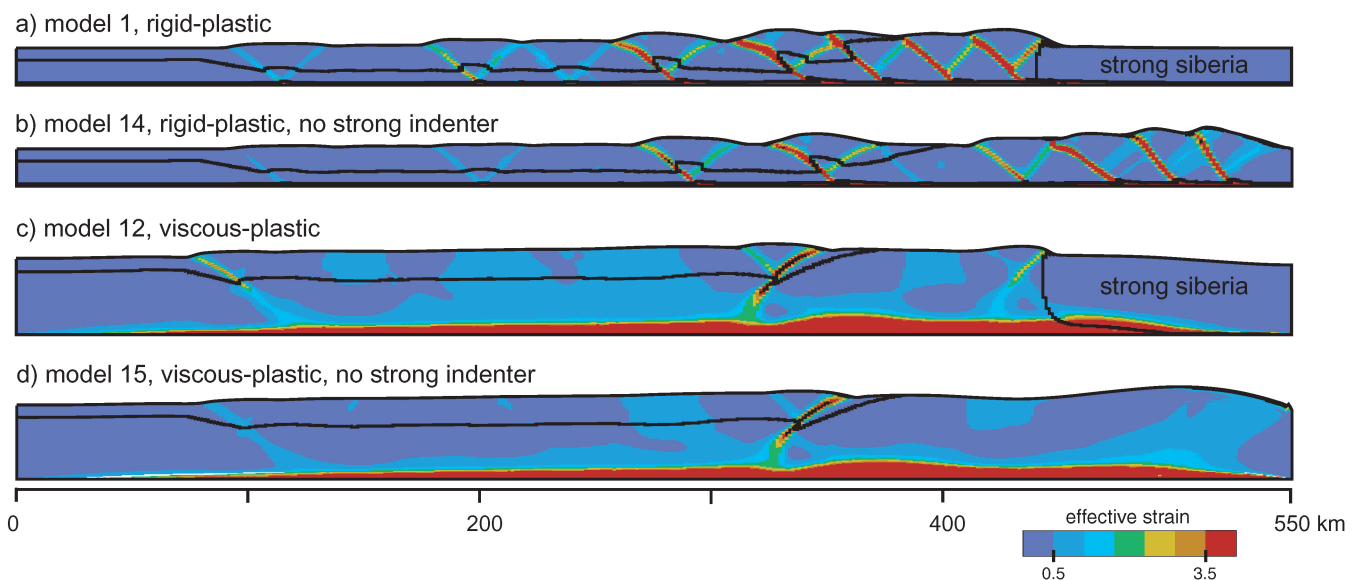


Figure 12. The role of the Siberian indenter in models with a rigid-plastic (a and b) and viscous-plastic (c and d) rheology. (a) Rigid-plastic reference model 1 with strong indenter, (b) identical model with standard strength Siberian crust (model 14), (c) Viscous-plastic model 12 with strong indenter and (d) identical model with standard strength Siberian crust (model 15). The flow law in (c) and (d) is for wet quartz (Gleason & Tullis 1995). A strong Siberian indenter transfers shortening efficiently to the basin area and suppresses thrusting in the domain of the west Siberian plate margin.

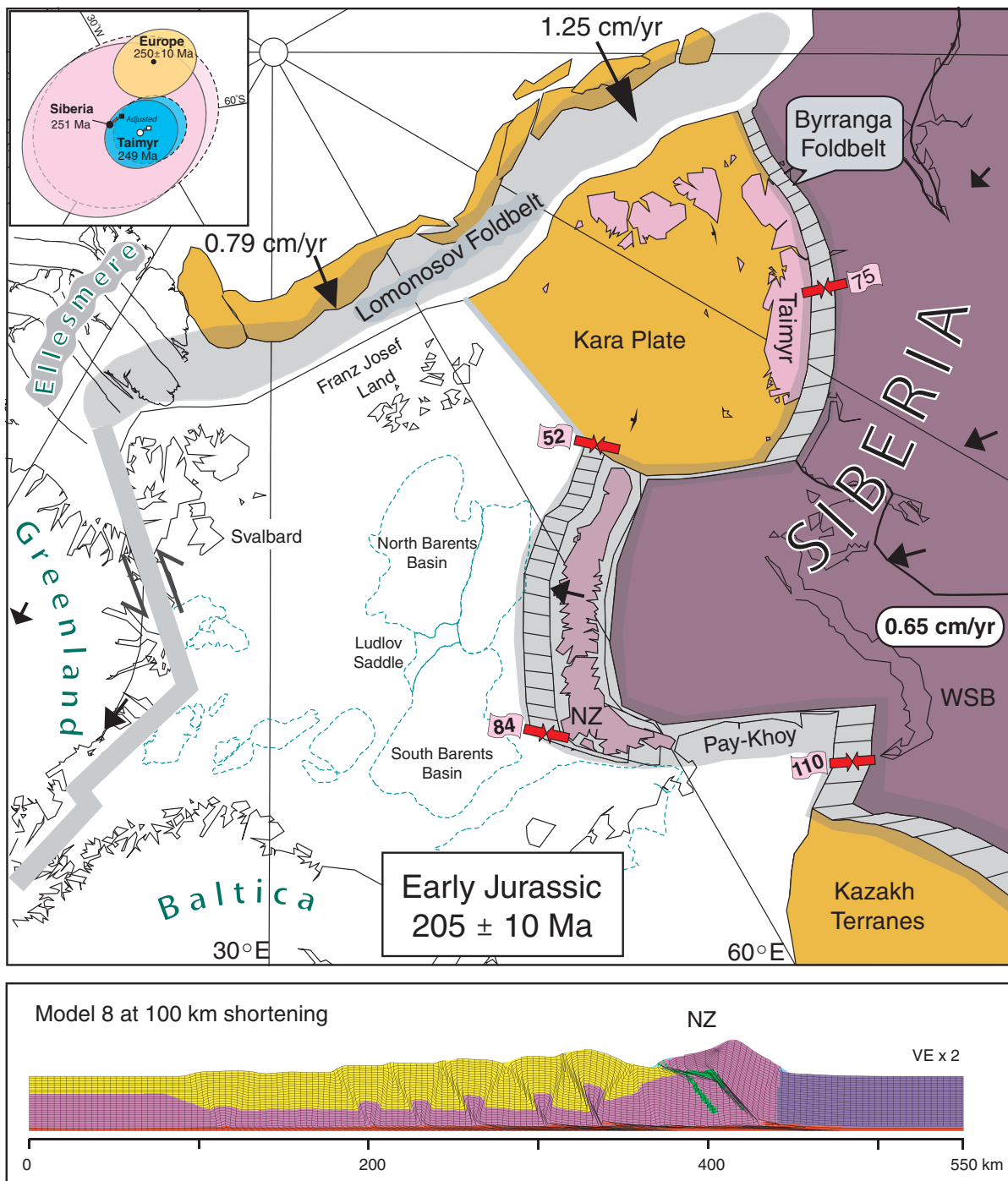


Figure 13. Plate reconstruction at *ca.* 205 Ma in which Baltica, with the Barents Sea, is kept fixed. The reconstruction is halfway through the Late Triassic–Early Jurassic compressional event and the Siberian plate has been pushed with around 100 km. The grey-shaded areas denotes areas that are affected by this deformation and the striped areas denote the subsequent difference between 205 and 190 Ma. The compressional arrows denote the stress-field direction, the numbers in the pink boxes represent the amount of subsequent compression (in km) that will occur and the single black arrows are point velocities. The compression leads to development of the Byrranga fold and thrust belt east of Taimyr. At the same time we anticipate that the Lomonosov terranes are colliding along the north Barents Sea margin, while the West Barents Sea margin is undergoing large-scale sinistral strike faulting (detailed in Torsvik *et al.* 2006). NZ = Novaya Zemlya; WSB = West Siberian Basin. The lower diagram shows our model 8 after 100 km of shortening. Pre-existing thrusts facilitate thrusting of Novaya Zemlya material over the eastern margin of the Barents Sea, while simultaneously thrusts develop in the Barents Sea basin. Top-left inset compares the *ca.* 250 Ma mean palaeomagnetic poles from Europe (50.5°S, 337.6°E; A95 = 5.3°; N = 8 poles), Siberia (55.7°S, 323.2°E; A95 = 12.2°; N = 3 poles) and Taimyr (59.2°S, 327.9°E; A95 = 4.7°; N = 2 poles) (see Cocks & Torsvik 2007, and references therein). The mean poles are plotted with 95 per cent confidence ovals (A95). Our plate tectonic reconstruction (with approximately 200 km post-250 Ma convergence in the Novaya Zemlya region) improves the correlation between Europe, Siberia and Taimyr. However, both the adjusted and the *in situ* pole for Siberia plot within the 95 per cent confidence oval of Europe. Conversely, the Taimyr *in situ* pole differs from the European one, but only around 100 km of convergence (Euler pole: 77°N, 144.6°E, angle = 2°) is needed to make the Taimyr and European pole overlap within their 95 per cent confidence oval. Based on these data, we, therefore, estimate that the displacement of the Siberian plate was 100 km at a minimum, but the upper estimate from the palaeomagnetic data exceeds 1000 km.

& Bailey (1995), Fig. 2), which could have been achieved along pre-existing shear zones inherited from older orogenies (Fig. 9). Shortening in our models is caused by the displacement of the Siberian plate which acts as an indenter. Part of the shortening is taken up by thrusts at Novaya Zemlya and the westward displacement of Novaya Zemlya will, therefore, be less than the westward displacement of the Siberian plate. A conservative estimate of the shortening that caused the westward movement of Novaya Zemlya and the inversion of the eastern Barents Sea basins based on our modelling results is 100–200 km.

Our models indicate that the westward displacement of Novaya Zemlya is less than in previous reconstructions. Fig. 13 shows a new plate reconstruction for the Barents Sea region at 205 Ma. The Siberian plate (along the eastern margin of Novaya Zemlya) is modelled to move with our maximum estimate of approximately 200 km between 220 and 190 Ma. The reconstruction is thus at a time when half of the shortening has taken place and the Siberian plate has been pushed approximately 100 km. The amount of shortening will naturally vary along the margin of Novaya Zemlya as the plate motion of Siberia is calculated as rotation around an Euler pole. The Euler rotation pole of the Siberian plate relative to Baltica at 220 Ma is given by 77°N latitude, 144.6°E longitude and a rotation angle of 5°, which yields a mean plate speed of 0.65 cm yr⁻¹. We use the same rotation pole for Novaya Zemlya relative to Baltica/Barents Sea, but with an angle of 4° at 220 Ma. This simulates compression at Novaya Zemlya while it is being thrust into the Barents Sea. The resulting westward displacement of Novaya Zemlya is between 100 and 170 km (from north to south) with a point velocity of around 0.5 cm yr⁻¹ at the centre of Novaya Zemlya (velocity vector in Fig. 13).

Palaeomagnetic data give a minimum estimate of 100 km convergence based on Euler poles that result in near orthogonal convergence at Novaya Zemlya and on the assumption that the Pay-Khoy region acted as a strike slip zone ('small circle'). However, the upper limit for allowable convergence exceeds 1000 km owing to the geometry of the Euler pole and the uncertainties in the mean poles for Europe, Siberia and Taimyr (Fig. 13). The large convergence estimates in Otto & Bailey (1995) and Torsvik & Andersen (2002), that is, 500–700 km, were motivated by a scenario in which Novaya Zemlya was first involved in the older Uralian Orogeny and thought to form a near-linear continuation of the Uralian Belt. It was subsequently thrust into the Barents Sea to reach its more westerly position. We assume that Novaya Zemlya already was in a more westerly position by Late Triassic–Early Jurassic times and speculate that it may not have been aligned with Taimyr and the Uralian Belt.

Our combination of numerical models and plate reconstructions has resulted in a first-order quantification of the amount of westward displacement of the Siberian plate margin and Novaya Zemlya in the Late Triassic–Early Jurassic. This interdisciplinary approach allows us to sharpen estimates of plate tectonic movements in areas where few constraints exist, while also yielding more insight into tectonic processes taking place at plate margins.

ACKNOWLEDGMENTS

The software used for the numerical calculations was initially developed by Ph. Fullsack and the Dalhousie Geodynamics Group. The plate reconstructions were made using SPlates, developed by the NGU Centre for Geodynamics. We thank Lykke Gemmer for helpful comments on the first version of this manuscript and Roy Gabrielsen and Conall Mac Niocaill for their constructive reviews. NFR, NGU

and Statoil ASA are thanked for financial support (PETROMAKS Frontier Science and Exploration no. 163395/S30).

REFERENCES

- Artemieva, I.M. & Mooney, W.D., 2001. Thermal thickness and evolution of Precambrian lithosphere: a global study, *J. geophys. Res.*, **106**, 16 387–16 414.
- Baturin, D., Vinogradov, A. & Yunov, A., 1991. Tectonics and hydrocarbon potential of the Barents Megatrough, Multiclient Report, Laboratory of Regional Geodynamics, LARGE International Moscow, Abstract, *Am. Ass. of Petr. Geol. Bull.*, **75**(8), 1404.
- Beaumont, C., Fullsack, P. & Hamilton, J., 1992. Erosional control of active compressional orogens, in *Thrust Tectonics*, pp. 1–19, ed. McClay, K.R., Chapman and Hall, New York.
- Beaumont, C., Kamp, P.J.J., Hamilton, J. & Fullsack, Ph., 1996. The continental collision zone, South Island, New Zealand: comparison of geodynamical models and observations, *J. geophys. Res.*, **101**, 3333–3359.
- Bos, B. & Spiers, C.J., 2002. Frictional-viscous flow of phyllosilicate-bearing fault rock: microphysical model and implications for crustal strength profiles, *J. geophys. Res.*, **107**, doi:10.1029/2001JB000301.
- Brown, D. & Ehtler, H., 2005. The Urals, *Encyclopedia Geol.*, **2**, 86–95.
- Brun, J.P. & Nalpas, T., 1996. Graben inversion in nature and experiments, *Tectonics*, **15**, 677–687.
- Buchanan, P.G. & McClay, K.R., 1991. Sandbox experiments of inverted listric and planar faults systems, *Tectonophysics*, **188**, 97–115.
- Bugge, T. *et al.*, 2002. Shallow stratigraphic drilling applied in hydrocarbon exploration of the Nordkapp Basin, Barents Sea, *Mar. Petr. Geol.*, **19**, 13–37.
- Buiter, S.J.H. & Pfiffner, O.A., 2003. Numerical models of the inversion of half-graben basins, *Tectonics*, **22**, doi: 10.1029/2002TC001417.
- Buiter, S.J.H., Babeyko, A.Yu., Ellis, S., Gerya, T.V., Kaus, B.J.P., Kellner, A., Schreurs, G. & Yamada, Y., 2006. The numerical sandbox: comparison of model results for a shortening and an extension experiment, in *Analogue and Numerical Modelling of Crustal-Scale Processes*, Vol. 253, pp. 29–64, eds Buiter, S.J.H. & Schreurs, G., Geol. Soc., Spec. Publ., London.
- Bungum, H., Ritzmann, O., Maercklin, N., Faleide, J.-I., Mooney, W.D. & Detweiler, S.T., 2005. Three-dimensional model for the crust and upper mantle in the Barents Sea region, *EOS, Trans. Am. geophys. Un.*, **86**, 160–161.
- Byerlee, J., 1978. Friction of rocks, *Pageoph.*, **116**, 615–626.
- Cocks, R.L.M. & Torsvik, T.H., 2005. Baltica from the late Precambrian to mid Palaeozoic: the gain and loss of a terrane's identity, *Earth-Sci. Rev.*, **72**, 39–66.
- Cocks, R.L.M. & Torsvik, T.H., 2007. Siberia, the wandering northern terrane, and its changing geography through the Palaeozoic, *Earth-Sci. Rev.*, **82**, 29–74.
- Cooper, M.A. *et al.*, 1989. Inversion tectonics—a discussion, in *Inversion Tectonics*, Vol. 44, pp. 335–347, eds Cooper, M.A. & Williams, G.D., Geol. Soc. Spec. Publ.
- Culling, W.E.H., 1960. Analytical theory of erosion, *J. Geol.*, **68**, 336–344.
- Dahlen, F.A., 1984. Noncohesive critical coulomb wedges: an exact solution, *J. geophys. Res.*, **89**, 10 125–10 133.
- Dahlen, F.A. & Barr, T.D., 1989. Brittle frictional mountain building 1. Deformation and mechanical energy budget, *J. geophys. Res.*, **94**, 3906–3922.
- Del Ventisette, C., Montanari, D., Sani, F. & Bonini, M., 2006. Basin inversion and fault reactivation in laboratory experiments, *J. Struct. Geol.*, **28**, 2067–2083.
- Eisenstadt, G. & Withjack, M.O., 1995. Estimating inversion: results from clay models, in *Basin Inversion*, Vol. 88, pp. 119–136, eds Buchanan, J.G. & Buchanan, P.G., Geol. Soc. Spec. Publ.
- Fullsack, Ph., 1995. An arbitrary Lagrangian-Eulerian formulation for creeping flows and its application in tectonic models, *Geophys. J. Int.*, **120**, 1–23.

- Gee, D.G., 2005. Scandinavian Caledonides (with Greenland), in *Encyclopedia of Geology*, Vol. 2, pp. 64–74, eds Selley, R.C., Cocks, L.R.M. & Plimer, I.R., Elsevier, Amsterdam.
- Gleason, G.C. & Tullis, J., 1995. A flow law for dislocation creep of quartz aggregates determined with the molten salt cell, *Tectonophysics*, **247**, 1–23.
- Hansen, D.L. & Nielsen, S.B., 2003. Why rifts invert in compression, *Tectonophysics*, **373**, 5–24.
- Hansen, D.L., Nielsen, S.B. & Lykke-Andersen, H., 2000. The post-Triassic evolution of the Sorgenfrei-Tornquist Zone—results from thermo-mechanical modelling, *Tectonophysics*, **328**, 245–267.
- Inger, S., Scott, R.A. & Golionko, B.G., 1999. Tectonic evolution of the Taimyr Peninsula, northern Russia: implications for Arctic continental assembly, *J. Geol. Soc., Lond.*, **156**, 1069–1072.
- Ivanova, N.M., Sakoulina, T.S. & Roslov, Yu. V., 2006. Deep seismic investigation across the Barents-Kara region and Novozemelskiy Fold Belt (Arctic Shelf), *Tectonophysics*, **420**, 123–140.
- Johansen, S.E. *et al.*, 1993. Hydrocarbon potential in the Barents Sea region: play distribution and potential, in *Arctic Geology and Petroleum Potential*, Vol. 2, pp. 273–320, eds Vorren, T.O., Bergsager, E. Dahl-Stamnes, Ø.A., Holter, E., Johansen, B., Lie, E. & Lund, T.B., NPF Spec. Publ.
- Koons, P.O., 1990. Two-sided orogen: collision and erosion from the sandbox to the Southern Alps, New Zealand, *Geology*, **18**, 679–682.
- McClay, K.R., 1995. The geometries and kinematics of inverted fault systems: a review of analogue model studies, in *Basin Inversion*, Vol. 88, pp. 97–118, eds Buchanan, J.G. & Buchanan, P.G., Geol. Soc. Spec. Publ.
- Mulugeta, G., 1988. Modelling the geometry of Coulomb thrust wedges, *J. Struct. Geol.*, **10**, 847–859.
- Natal'in, B.A. & Şengör, A.M.C., 2005. Late Paleozoic to Triassic evolution of the Turan and Skythian platforms: the pre-history of the paleo-Tethyan closure, *Tectonophysics*, **404**, 175–202.
- Nikishin, A.M., Ziegler, P.A., Abbott, D., Brunet, M.-F. & Cloetingh, S., 2002. Permo-Triassic intraplate magmatism and rifting in Eurasia: implication for mantle plumes and mantle dynamics, *Tectonophysics*, **351**, 3–39.
- Northrup, C.J., Royden, L.H. & Burchfiel, B.C., 1995. Motion of the Pacific plate relative to Eurasia and its potential relation to Cenozoic extension along the eastern margin of Eurasia, *Geology*, **23**, 719–722.
- O'Leary, N., White, N., Tull, S., Bashilov, V., Kuprin, V., Natapov, L. & MacDonald, D., 2004. Evolution of the Timan-Pechora and South Barents Sea basins, *Geol. Mag.*, **151**, 141–160.
- Otto, S.C. & Bailey, R.J., 1995. Tectonic evolution of the northern Ural Orogen, *J. Geol. Soc. Lond.*, **152**, 903–906.
- Panien, M., Schreurs, G. & Pfiffner, O.A., 2005. Sandbox experiments on basin inversion: testing the influence of basin orientation and basin fill, *J. Struct. Geol.*, **27**, 433–445.
- Panien, M., Buiter, S.J.H., Schreurs, G. & Pfiffner, O.A., 2006. Inversion of a symmetric basin: insights from a comparison between analogue and numerical experiments, in *Analogue and Numerical Modelling of Crustal-Scale Processes*, Vol. 253, pp. 253–270, eds Buiter, S.J.H. & Schreurs, G., Geol. Soc. Spec. Publ., London.
- Pysklywec, R.N., 2006. Surface erosion control on the evolution of the deep lithosphere, *Geology*, **34**, 225–228.
- Ranalli, G., 1987. *Rheology of the Earth*, 366 pp., Allen and Unwin Inc., Winchester, USA.
- Ritzmann, O., Maercklin, N., Faleide, J.I., Bungum, H., Mooney, W.D. & Detweiler, S.T., 2007. A three-dimensional geophysical model of the crust in the Barents Sea region: model construction and basement characterization, *Geophys. J. Int.*, **170**, 417–435.
- Roberts, D. & Olovyanishnikov, V., 2004. Structural and tectonic development of the Timanide orogen, in *The Neoproterozoic Timanide Orogen of Eastern Baltica*, Vol. 30, pp. 47–57, eds Gee, D.G. & Pease, V., Geol. Soc., London, Mem.
- Rybacki, E. & Dresen, G., 2000. Dislocation and diffusion creep of synthetic anorthite aggregates, *J. geophys. Res.*, **105**, 26 017–26 036.
- Sandiford, M., 1999. Mechanics of basin inversion, *Tectonophysics*, **305**, 109–120.
- Schreurs, G., Hänni, R. & Vock, P., 2001. Four-dimensional analysis of analog models: experiments on transfer zones in fold and thrust belts, *Geol. Soc. Am. Mem.*, **193**, 179–190.
- Simpson, G.D.H., 2006. Modelling interactions between fold-thrust belt deformation, foreland flexure and surface mass transport, *Basin Res.*, **18**, 125–143.
- Storti, F., Salvini, F. & McClay, K., 2000. Synchronous and velocity-partitioned thrusting and thrust polarity reversal in experimentally produced, doubly-vergent thrust wedges: implications for natural orogens, *Tectonics*, **19**, 379–396.
- Torsvik, T.H. & Andersen, T.B., 2002. The Taimyr fold belt, Arctic Siberia: timing of pre-fold remagnetisation and regional tectonics, *Tectonophysics*, **352**, 335–348.
- Torsvik, T.H., Gaina, C., Steinberg, M. & Van der Voo, R., 2006. North Atlantic fits with implications for the Barents Sea, in NGU Report 2006.077 (confidential)
- Van der Voo, R., Levashkova, N.M., Skrinnik, L.I., Kara, T.V. & Bazhenov, M.L., 2006. Late orogenic, large-scale rotations in the Tien Shan and adjacent mobile belts in Kyrgyzstan and Kazakhstan, *Tectonophysics*, **426**, 335–360.
- Vernikovsky, V.A., 1996. The geodynamic evolution of the Taimyr folded area, *Geol. Pac. Ocean*, **12**, 691–704.
- Vernikovsky, V.A., 1997. Neoproterozoic and late Paleozoic Taimyr Orogenic and ophiolitic belts, North Asia: a review and models for their formation, *Proc. 30th Int. Geol. Congr., Beijing, China*, vol. 7, 121–138.
- Vyssotski, A.V., Vyssotski, V.N. & Nezhdanov, A.A., 2006. Evolution of the West Siberian Basin, *Mar. Petr. Geol.*, **23**, 93–126.
- Walderhaug, H.J., Eide, E.A., Scott, R.A., Inger, S. & Golionko, E.G., 2005. Palaeomagnetism and $^{40}\text{Ar}/^{39}\text{Ar}$ geochronology from the South Taimyr igneous complex, Arctic Russia: a Middle-Late Triassic magmatic pulse after Siberian flood-basalt volcanism, *Geophys. J. Int.*, **163**, 501–517.
- Willett, S.D., 1999. Orogeny and orography: the effects of erosion on the structure of mountain belts, *J. geophys. Res.*, **104**, 28 957–28 981.
- Wilson, D.S., 1996. Fastest know spreading on the Miocene Cocos-Pacific plate boundary, *Geophys. Res. Lett.*, **23**, 3003–3006.
- Ziegler, P.A., 1989. *Evolution of Laurussia: A Study in Late Palaeozoic Plate Tectonics*, 102 pp., Kluwer Academic Publishers, Dordrecht, The Netherlands.
- Ziegler, P.A., Cloetingh, S. & van Wees, J.-D., 1995. Dynamics of intra-plate compressional deformation: the Alpine foreland and other examples, *Tectonophysics*, **252**, 7–59.